Stabilized thin film heterostructure for electrochemical applications.

Esposito, Vincenzo; Sanna, Simone; Pryds, Nini; Linderoth, Søren

Publication date:
2015

Document Version
Publisher's PDF, also known as Version of record

(12) INTERNATIONAL APPLICATION PUBLISHED UNDER THE PATENT COOPERATION TREATY (PCT)

(19) World Intellectual Property Organization
International Bureau

(43) International Publication Date
15 January 2015 (15.01.2015)

WIPO | PCT

(10) International Publication Number
WO 2015/004237 A1

(51) International Patent Classification:
H01M 8/12 (2006.01) *H01M 8/02* (2006.01)

(21) International Application Number:
PCT/EP2014/064812

(22) International Filing Date:
10 July 2014 (10.07.2014)

(25) Filing Language: English

(26) Publication Language: English

(30) Priority Data:
13175901.1 10 July 2013 (10.07.2013) EP

(71) Applicant: **DANMARKS TEKNISKE UNIVERSITET** [DK/DK]; Anker Engelunds Vej 1, DK-2800 Kgs. Lyngby (DK).

(72) Inventors: **ESPOSITO, Vincenzo**; Tegelgårdsgatan 24, S-21133 Malmø (SE). **SANNA, Simone**; Peter Bangs Vej 135, 2. tv., DK-2000 Frederiksberg (DK). **PRYDS, Nini**; Peter Petersens Allé 39, DK-2791 Dragør (DK). **LINDEROTH, Søren**; Egevej 47, DK-4000 Roskilde (DK).

(74) Agents: **THORSEN, Jesper** et al.; Inspicos A/S, P.O. Box 45, Kogle Allé 2, DK-2970 Hørsholm (DK).

(81) Designated States *(unless otherwise indicated, for every kind of national protection available)*: AE, AG, AL, AM, AO, AT, AU, AZ, BA, BB, BG, BH, BN, BR, BW, BY, BZ, CA, CH, CL, CN, CO, CR, CU, CZ, DE, DK, DM, DO, DZ, EC, EE, EG, ES, FI, GB, GD, GE, GH, GM, GT, HN, HR, HU, ID, IL, IN, IR, IS, JP, KE, KG, KN, KP, KR, KZ, LA, LC, LK, LR, LS, LT, LU, LY, MA, MD, ME, MG, MK, MN, MW, MX, MY, MZ, NA, NG, NI, NO, NZ, OM, PA, PE, PG, PH, PL, PT, QA, RO, RS, RU, RW, SA, SC, SD, SE, SG, SK, SL, SM, ST, SV, SY, TH, TJ, TM, TN, TR, TT, TZ, UA, UG, US, UZ, VC, VN, ZA, ZM, ZW.

(84) Designated States *(unless otherwise indicated, for every kind of regional protection available)*: ARIPO (BW, GH, GM, KE, LR, LS, MW, MZ, NA, RW, SD, SL, SZ, TZ, UG, ZM, ZW), Eurasian (AM, AZ, BY, KG, KZ, RU, TJ, TM), European (AL, AT, BE, BG, CH, CY, CZ, DE, DK, EE, ES, FI, FR, GB, GR, HR, HU, IE, IS, IT, LT, LU, LV, MC, MK, MT, NL, NO, PL, PT, RO, RS, SE, SI, SK, SM, TR), OAPI (BF, BJ, CF, CG, CI, CM, GA, GN, GQ, GW, KM, ML, MR, NE, SN, TD, TG).

Declarations under Rule 4.17:

— *of inventorship (Rule 4.17(iv))*

Published:

— *with international search report (Art. 21(3))*

WO 2015/004237 A1

(54) Title: STABILIZED THIN FILM HETEROSTRUCTURE FOR ELECTROCHEMICAL APPLICATIONS

(57) Abstract: The invention provides a method for the formation of a thin film multi-layered heterostructure upon a substrate, said method comprising the steps of: a. providing a substrate; b. depositing a buffer layer upon said substrate, said buffer layer being a layer of stable ionic conductor (B); c. depositing a layer A upon said buffer layer, said layer A being a layer of fast ionic conductor (A), said layer A having a thickness (t_A) of 20 nm or less; d. depositing a layer B upon said layer A, said layer B being a layer of stable ionic conductor (B), said layer B having a thickness (t_B) of 150 nm or less; and e. repeating steps b. and c. a total of N times, such that N repeating pairs of layers (A/B) are built up, wherein N is 1 or more. The invention also provides a thin film multi-layered heterostructure as such, and the combination of a thin film multi-layered heterostructure and a substrate. The heterostructure finds use as an electroceramic, in particular in SOFCs.

STABILIZED THIN FILM HETEROSTRUCTURE FOR ELECTROCHEMICAL APPLICATIONS

FIELD OF THE INVENTION

The present invention relates to a method for the formation of a thin film multi-layered heterostructure upon a substrate. The invention also provides a thin film multi-layered heterostructure as such, and the combination of a thin film multi-layered heterostructure and a substrate. The heterostructure finds use as an electroceramic, in particular as an electrolyte in Solid Oxide Fuel Cells (SOFCs).

BACKGROUND OF THE INVENTION

Solid state ionic conductors, or ionics, are materials which can conduct electric charges via fast defect migration mechanisms in their structure. Among the different ionics, oxygen defect conductors are crystalline metal oxide compounds, i.e. electroceramics, which provide outstanding electronic performances. These are used as key components in several strategic technologies such as fuel cells, membranes, batteries, gas sensors, in hydrolysis devices, etc..

Since electric conductivity in electroceramics strictly depends on diffusive phenomena, i.e. defect formation and migration, the best performing ionic conductors generally also present poor phase stability, high reactivity with other materials, and fast degradation at operative conditions, such as at low oxygen partial pressures and at high temperatures. Conversely, stable electroceramics have usually better chemical stability but their electrical performances are limited to applications in highly diffusive regimes at high temperatures. Efforts have been made to provide ceramic materials with advantageous electrical properties and – at the same time – relatively good chemical stability, but success has been limited.

US 2011/0200910 and WO 97/41612 disclose an SOFC with a bilayer electrolyte comprising a cerium oxide layer and a bismuth oxide layer. The layers are deposited via Pulsed Laser Deposition (PLD), and are in the order of 4-10 nm thick. Only bilayer electrolytes are described.

US 2006/0210706 discloses a thin-film SOFC. The ytthria stabilized zirconia (YSZ) electrolyte by PLD layer may be 0.01 μm-10 μm. These films may be used in fields other than SOFCs.

WO 2007/011894 discloses Physical Vapor Deposition (PVD) deposited nano-composites, primarily for use as electrodes. The nanocomposites comprise interpenetrating networks of electronic conductor (metal) and ionic conductor (ceramic).

Efforts are being made over the years to lower SOFC operating temperatures to 500-700 °C in order to reduce cost and improve reliability and operational life. Reduction of the SOFC operating temperature results in less degradation of cell and stack components but require use of new materials and changing of processing techniques to thin film deposition. At lower temperatures, electrolyte conductivity decreases significantly. Therefore the ohmic losses from the electrolyte can be minimized either by the use of new materials with higher conductivity and/or through reduction of the thickness of the electrolyte, or both.

There is therefore still a need for thin film electroceramic materials, and routes to said materials, which can simultaneously provide both good ionic conductivity and high stability in the same material.

SUMMARY OF THE INVENTION

In a first aspect the present invention relates to a method for the formation of a thin film multi-layered heterostructure upon a substrate, said method comprising the steps of:

a. providing a substrate;

b. depositing a buffer layer upon said substrate, said buffer layer being a layer of stable ionic conductor (B);

c. depositing a layer A upon said buffer layer, said layer A being a layer of fast ionic conductor (A), said layer A having a thickness (tA) of 20 nm or less;

d. depositing a layer B upon said layer A, said layer B being a layer of stable ionic conductor (B), said layer B having a thickness (tB) of 150 nm or less; and

e. repeating steps c. and d. a total of N times, such that N repeating pairs of layers (A/B) are built up, wherein N is 1 or more.

Suitably, N is 2 or more, such as e.g. 6 or more, 10 or more, 15 or more or 20 or more.

The present invention also relates to a thin film multi-layered heterostructure comprising alternating layers of fast ionic conductor (A) and stable ionic conductor (B), wherein said layer of fast ionic conductor (A) has a thickness of 20 nm or less, and said layer of stable conductor (B) has a thickness of 150 nm or less; said heterostructure comprising N repeating pairs of layers (A/B), wherein N is 4 or more.

The invention also provides a combination of the thin film multi-layered heterostructure according to the invention and a substrate, and optionally a buffer layer located between said heterostructure and said substrate, wherein said fast ionic conductor (A) of said heterostructure is located adjacent said buffer layer.

A further aspect of the invention involves the use of a thin film multi-layered heterostructure according to the invention as a component of a solid-oxide fuel cell (SOFC), solid-oxide electrochemical cell (SOEC), gas-separation membrane, oxygen transport membrane (OTM), sensor or catalyst.

Additionally, the invention provides a solid-oxide fuel cell (SOFC) comprising the thin film multi-layered heterostructure of the invention as electrolyte.

Further aspects of the invention are to be found in the dependent claims.

LEGENDS TO THE FIGURES

Figure 1 shows schematically the portion of the thin film heterostructure, where the formula $S/S'/[A/B]_N$ represents the number of A/B number of repetition (N) deposited on the substrate (S) and buffer-layer (S'), the bilayer-(A/B)-repetition thickness (Λ), and the total thickness of the system (T_{tot}).

Figure 2 shows XRD θ-2θ patterns for superlattices GDC/[ESB/GDC]N/MgO having N=1, 10 and 20 with the same overall thickness (about 50 nm). The inset shows the rocking curve for superlattice having N=20. The diffraction pattern shows that two separate peaks related to individual layer at N=1 overlap at N>10, indicating the formation of a superstructure. The rocking curve at 1.3 ° in the inset indicates a high degree of in-plane structural order at the heterostructure.

Figure 3 shows TEM images of the multilayer GDC/[ESB/GDC]N/MgO film at N=20:.a) TEM image of hetero structure supported on MgO. b) Line plot of the pixel intensity from the TEM image (a) along the direction and at the horizontal position indicate by the arrow in figure (a). The plot is integrated over the full image height. c) HRTEM image of the hetero structure-MgO interface. d) Forward Fourier transformation of the HRTEM image (c). Real space distances for selected spots are indicated. e) Inverse Fourier transformation from spots corresponding to real space distances = 2.2 Å. f) Inverse Fourier transformation from spots corresponding to real space distances = 2.7 Å. g) Diffraction pattern from area covering both hetero structure and MgO. Real space distances for selected spots are indicated

Figure 4a and b show Arrhenius plot of conductivity taken in air (pO_2 = 0.21 atm) for multilayer GDC/[ESB/GDC]N/MgO films at diverse N = 1,...20 (Figure 4a) and for N=20, CeO_2 and for GDC/ESB thickness ratio 1:6 (Figure 4b). The plot shows that total electric conductivity depends on the number of the interfaces and on the composition of the layers. For a constant thickness of 50 nm, samples with N= 20 show max conductivity.

Figure 5a and 5b show Arrhenius plots of conductivity taken in H_2/N_2 mixture ($pO_2 = 10^{-18}$ atm) for multilayer GDC/[ESB/GDC]N/MgO films at diverse N = 1,...20 (figure 5a) and for N=20, CeO_2 and for GDC/ESB thickness ratio 1:6 (figure 5b). The plots show that total electric conductivity increase abruptly with a reversible at temperatures around 500-600 °C. Samples with thicker ESB layer undergo to fast degradation under reducing conditions.

Figure 6: Electrical conductivity properties of GDC/$[ESB/GDC]_{20}$/MgO sample as function of the oxygen partial pressure. Different pO_2 values were obtained by mixing O_2, H_2 and N_2 in different ratio in dry conditions. Particularly the sample was tested at three different temperatures: at 450 °C < T_t, at 550°C ≈ T_t, and at 650 °C > T_t.

Figure 7 shows conductivity performances with time (a) and redox cycles (b) for multilayer system samples at N=20 (ageing tests). Samples do not present ageing phenomena usually observed in Bi_2O_3 materials. Multilayer is stable for several hours at different temperatures (500, 400, 500, 600 °C). Cyclic test shows that multilayer N=20 preserve electrical properties under several oxidative and reducing condition and after 18 hours in reducing conditions.

Figure 8 shows shows a micrograph of a GDC/ESB heterostructure with N=1. A fracture cross section of the heterostructure is shown, after operation as SOFC in H_2/Air at 600 °C. The ESB layer of ca. 200 nm has degraded showing porosity and lack of material.

Figure 9 shows a fracture cross section of the GDC/ESB heterostructure N=2 after operation as SOFC in H_2/Air at 600 °C. The ESB layer of below 5 nm has not degraded. The resulting film was highly coherent with no delamination at the ESB/C

DETAILED DISCLOSURE OF THE INVENTION

Definitions

"Fast ionic conductors" refers to materials which have high charge mobility and thus high conductivity. In the context of the present invention, the term "fast ionic conductor" is used to mean electroceramic pure ionic conductors and mixed electronic-ionic conductors with a conductivity at the operating temperature (Top) that is at least equivalent in magnitude to proton conduction in a strong acid: 10^{-1} S cm^{-1} at Top [as measured in *J.B. Goodenough, Proc. R. Soc. Lond. A 393, 215-234, 1984.*]. This value is above the typical ionic conductivity of cubic stabilized -ZrO_2 phase at Top = 500-700 °C.

In the context of the present invention, the term "stable ionic conductor" is used to mean materials which are inert toward gas and other solid used in the operative conditions. Particularly, stable ionic conductors preserve phase, chemical composition, and have similar electrical properties, both when they are processed and operate in physical contact with other materials, e.g. support, electrodes, functional layers, and when they are processed and operate in oxidant mixture and reducing gases mixtures,, such as fuel mixtures at low oxygen partial pressure (pO_2). Particularly, the phase and chemical composition stability of a generic metal oxide compound $A_nB_mO_{k-x}$ (A and B are metals) has the property of maintaining the same stoichiometric composition of the starting elements (m, n and k constant) with a possible reversible change in the oxygen content (x) due to changes of oxygen vacancy content at the processing and operating conditions. As an example, a "stable ionic conductor" is preserved as a single phase during fuel cell operation (e.g. T >400ºC, pO_2 greater or equal to 10^{-32}atm at the fuel side).

A superlattice is a material with periodically alternating layers of several crystalline substances. Typically, the thickness of one layer is several nanometers. This leads to unique properties other then the constituent materials of the individual layers. By changing the material in each layer and the layer thickness it is often possible to optimize the desire properties of the system. The characteristic length scales in superlattices are: (1) the modulation wavelength, (2) the lattice spacing and (3) the structure coherence length.

Heterostruture is here defined as the material resulting from joining different crystalline substance. Periodic repetition of a heterostructure is equivalent to a superlattice.

Specific embodiments of the invention

The inventors have designed a set of multilayers where fast but unstable materials can be confined in the nano-range layer thickness by another layer. This is done in a manner such that the fast conductor is chemically encapsulated and protected by the stable conductors. Compositions and conditions to achieve this have been described.

The solution provided by the present invention requires reducing the thickness of the layered materials to the nanoscale. Results actually show that ESB decomposes althought the thickness is around 20-50 nm and even though the CGO is in the range of 100 nm and more. This means that there is a strict way to confine the fast materials into the heterostructure and it is not just a random layers thicknesses. On this latter point the invention differs from the state of the art defined by US 2011/0200910 and WO 97/41612 and others, in which only chemical protection in the micro-range is considered. This does not hold under reducing and oxidizing conditions. Similar considerations can be made for the electrical properties. A maximum conductivity for N = 20 has been achieved for film of total thickness of 300 nm, and it has been shown that for N = 30 the performance decreases.

Some of the materials used are usually not considered as electrolyte materials because they decompose at low pO_2. Good examples are $SrCoO_3$ and LSC, which are generally used as cathodes or membranes operating at high pO_2.

The above is evidence that is not just a matter of putting the materials together but in defining certain combinations of material properties, arrangements and thicknesses

In a first embodiment, therefore, the invention provides a method for the formation of a thin film multi-layered heterostructure. The thin film multi-layered heterostructure (also called "heterostructure" in this specification) is illustrated schematically in Figure 1. As stated above, the formula $S/S'/[A/B]_N$ represents the number of A/B number of repetition (N) deposited on the substrate (S) and buffer-layer (S'), the bilayer-(A/B)-repetition thickness (Λ), and the total thickness of the system (T_{tot}). The number of interfaces formed in the heterostructure is n = 2 x N.

The first main step of the method requires the provision of a substrate, upon which the thin film multi-layered heterostructure is formed. Suitable substrates should be either single- or poly-crystalline and have limited porosity (<5%), smooth surface (<500 nm), and chemical stability. A substrate used in the present invention is MgO single-crystal, which shows chemical stability, low electrical conductivity at high temperatures and it is thus ideal for the electrical characterization of the heterostructures. Other suitable substrates for real

applications include both polycrystalline and single crystals of Ni, other electroceramics with several dopant and stabilizers elements used in solid oxides-based electrochemical technologies (e.g. NiO, $SrTiO_3$ (STO), cubic-phase-stabilized-ZrO_2 (e.g. Y_2O_3-stabilized-ZrO_2 (YSZ)), $LaAlO_3$ (LAO), $LaSrCoO_3$ (LSC), $LaSrMnO_3$ (LSM), $(Ba,Sr)(CoFe)O_3$ (BSCF); $(La,Sr)(Co,Fe)O_3$ (LSCF), $SmSrCoO_3$ (SSC), $NdGaO_3$ (NGO), $SrRuO_3$ (SRO), CeO_2, doped Ceria (e.g. Gd_2O_3-doped-CeO_2, (GDC)) and other SOFC ceramic-metallic composites (CERMETS) for anode applications such as Ni-YSZ, Cu-YSZ, Zn-YSZ and similar). This also includes substrates for micro-SOFC such as Si, SiN, Forturan ®, sapphire, anodized alumina, TiO_2, and amorphous materials such as technical glasses and photo-etchable and conductive glasses.

The substrate is typically prepared by standard ceramic processing techniques (e.g. pressing, extrusion, spark plasma sintering (SPS), tape-casting, screen-printing, 3D printing, dip-coating, spin-coating, electrical anodization methods, etc.), or single crystal production methods.

In the second main step of the method, a buffer layer is provided on said substrate, typically by deposition techniques. The buffer layer is a layer used to achieve structural and chemical compatibility between the substrate and the first layer, and to isolate the fast ionic conductor (A) from the substrate. The buffer layer is a layer of stable ionic conductor (B). In particular embodiments, the buffer layer may be selected from MgO, NiO, STO, CGO, LAO, NGO and SRO. This is also illustrated in Figure 1. Preferably, the stable ionic conductor (B) in the buffer layer is the same as the stable ionic conductor (B) used as layer B.

In the third main step of the method a layer A is deposited upon the buffer layer. Deposition of layer A on the substrate/buffer layer typically takes place via a physical vapour deposition (PVD) technique selected independently from pulsed laser deposition (PLD), sputtering and atomic layer deposition (ALD), spray-pyrolysis, plasma assisted deposition, Chemical vapour deposition (CVD), and Electrodeposition (ED) methods or any other method for thin film fabrication.

Layer A is a layer of fast ionic conductor (A), as defined above. Fast ionic conductor (A) is a ceramic material, and preferred materials for the fast ionic conductor (A) are selected from pure ionic conductors and mixed electronic-ionic conductors such as Bi_2O_3 and cubic-stabilized bismuth oxide phases (i.e. doped with Er, Dy, Y, W, and their combinations in different molar amounts), Er-Stabilized Bi_2O_3 (ESB), stabilised cubic bismuth oxide (δ-Bi_2O_3), $(La_{1-x}Sr_x)CoO_3$, $(La_{1-x}Sr_x)(Co_{1-y}Fe_y)O_3$, , $La_{1-x}Sr_xGa_{1-y}Mg_yO_3$ (LSGM), $(AE_{1-x}Sr_x)(Co_{1-y},Fe_y)O_3$or $(AE_{1-x}Ba_x)(Ce_{1-z}Y_z)O_3$ (AE= alkaline earths: Ba, Sr)

The layers of the thin film multi-layered heterostructure are thin, on the nanometre scale. The layer A therefore has a thickness (t_A) of 20 nm or less, preferably 5 nm or less, more preferably 3 nm or less.

In the fourth main step of the method of the invention, a layer B is deposited upon said layer A. In a similar way to the layer A, deposition of layer B on layer A typically takes place via a physical vapour deposition (PVD) technique selected independently from pulsed laser deposition (PLD), sputtering and atomic layer deposition (ALD), spray-pyrolysis, plasma assisted deposition, Chemical vapour deposition (CVD), and Electrodeposition (ED) methods or any other method for thin film fabrication.

Layer B is a layer of stable ionic conductor (B), as defined above. Stable ionic conductor (B) is a ceramic material. The stable ionic conductor (B) is suitably selected from gadolinium doped oxide (GDC or CGO), acceptor doped-ceria compounds and acceptor co-doped-CeO_2 (doped-CeO_2), cubic-phase-stabilised-ZrO_2 or $Ba_{1-x}Sr_xZr_{1-z}Y_zO_3$.

Layer B has a thickness (t_B) of 150 nm or less, preferably 100 nm or less, more preferably 50 nm or less.

In a preferred embodiment, layers A and B have different thicknesses.The layer A may be thinner than layer B, such that the thickness ratio (t_A/t_B) is between 1:1 and 1:6. The heterostructure functions best when the stable material B is thicker; e.g. when the thickness ratio (t_A/t_B) is between 1:2 and 1:6.

It is preferred that fast ionic conductor (A) and stable ionic conductor (B) have the same, similar or compatible, crystal structure. Compatible crystal structures are those structures which – when deposited one on the top of the other – are continuous with limited lattice strain and no delamination. In this way, a certain amount of compatibility between the layers A and B can be achieved. Suitably, fast ionic conductor (A) and stable ionic conductor (B) are both ceramics with a fluorite crystal structure. Alternatively, fast ionic conductor (A) and stable ionic conductor (B) are both ceramics with a perovskite crystal structure. As another alternative, one conductor (A or B) is a ceramic with a fluorite crystal structure and the other conductor (B or A) is a ceramic with a perovskite crystal structure.

The following material combinations for A and B are of particular interest:

	A	**B**
i.	ESB	GDC
ii.	stabilised δ-Bi_2O_3	doped-CeO_2
iii.	LSC and LSCF	doped-CeO_2 and cubic-phase-stabilised-ZrO_2
iv	LSGM	doped-CeO_2 or cubic-phase-stabilised-ZrO_2
v.	(AE,Sr)(Co,Fe)O_3	cubic-phase-stabilised-ZrO_2
vi.	(AE,Sr)(Co,Fe)O_3	doped-CeO_2
vii.	$Ba_{1-x}Sr_xCe_{1-z}Y_zO_3$	$Ba_{1-x}Sr_xZr_{1-z}Y_zO_3$

In a preferred aspect, layer A is ESB, and layer B is CGO.

The third and fourth main steps of the invention are repeated a total of N times, such that N repeating pairs of layers (A/B) are built up. In particular, N is 1 or more. Suitably, N is 5 or more, such as e.g. 6 or more, 10 or more, 15 or more or 20 or more. The preferred upper limit for N is 30.

The combination of the thin layers A and B and the repetitive structure of the thin film multi-layered heterostructure provides a single material which has the beneficial properties of the fast ionic conductor (A) and the stable ionic conductor (B), as the two types of conductors are mixed at the atomic level. This is discussed in detail with respect to the data illustrated in Figures 2-7.

In particular, the inventors have discovered that – if the layer A is too thick (above 50 nm), it becomes unstable, and degrades when the heterostructure is used in an SOFC. As shown in Figure 8, an ESB layer of ca. 200 nm degrades under operation in an SOFC, while very thin ESB layers (ca. 5 nm in Figure 9) do not.

The thin film multi-layered heterostructure has a total thickness T_{tot} of 50 nm or more, preferably 100 nm or more, more preferably 200 nm or more.

The method of the invention may additionally comprise the step of at least partially removing the substrate from the thin film multi-layered heterostructure by chemical reduction of metal oxide to metallic form with formation of connected porosity, chemical dissolution of transition metal component by leaching, selective etching of the substrate by photo-chemical methods and mechanical methods. Selective etching is intended as the practice to remove the substrate in selected areas in one side of the film, preserving a continuous framework of the substrate for mechanical and structural functions. This means that the thin film multi-layered heterostructure can be accessed from both sides and substrate supports mechanically the film on the substrate.

In a second embodiment, the invention provides a thin film multi-layered heterostructure comprising alternating layers of fast ionic conductor (A) and stable ionic conductor (B), wherein said layer of fast ionic conductor (A) has a thickness of 20 nm or less, and said layer of stable conductor (B) has a thickness of 100 nm or less; said heterostructure comprising N repeating pairs of layers (A/B), wherein N is 1 or more.

All details of the thin film multi-layered heterostructure and the layers A and B provided above for the method of the invention are also relevant for the heterostructure itself. In particular, the material combinations for A and B i-vi listed above are of particular interest. Layers A and B are ceramic materials. In a preferred aspect of this embodiment, layer A is ESB, and layer B is CGO. The heterostructure preferably has a total thickness of 50 nm or more, preferably 100 nm or more, more preferably 200 nm or more. In particular, the said heterostructure comprises N repeating pairs of layers (A/B), wherein N is 5 or more, such as e.g. 6 or more, 10 or more, 15 or more or 20 or more.

In a third embodiment, a combination of the thin film multi-layered heterostructure according to the invention and a substrate, and optionally a buffer layer located between said heterostructure and said substrate, is provided. In this combination, the stable ionic conductor (B) of said heterostructure is located adjacent said substrate or – when present – said buffer layer. Again, all details of the thin film multi-layered heterostructure and the layers A and B provided above for the method of the invention are also relevant for the combination of heterostructure and substrate in this embodiment.

The thin film multi-layered heterostructure according to the invention finds use as a component of a solid-oxide fuel cell (SOFC), solid-oxide electrochemical cell (SOEC), gas-separation membrane, oxygen transport membrane (OTM), sensor or catalyst. In particular, the heterostructure of the invention can be used in high temperature sensors or catalysts for gas detection or conversion (e.g. NO_x, SO_x, O_2, CO_x etc).

In particular, the thin-film multi-layered heterostructure is particularly suited for use as an electrolyte in an SOFC. The invention thus provides a solid-oxide fuel cell (SOFC) comprising the thin film multi-layered heterostructure of the invention as electrolyte. In such an SOFC, the support is partially chemically etched or mechanically removed at suitable locations, leaving the heterostructure exposed to the gas on both sides. Heterostrutures deposited on CERMET where the starting dense metal oxide phase is reduced by hydrogen into metallic form with formation of pores. Another alternative solution for the cermet substrate is that the transition metal component is removed by selective chemical etching (leaching) to open the suitable porosity at the substrate side.

EXAMPLE

To illustrate the invention, thin film heterostructures made of alternate layers of 20 mol% gadolinium-doped ceria ($Ce_{0.8}Gd_{0.2}O_{2-\delta}$, GDC) and 20% erbium-stabilized bismuth oxide ($Bi_{0.8}Er_{0.2}O_{2-\delta}$, ESB), were fabricated by pulsed laser deposition (PLD) onto MgO substrates. Different architectures are deposited keeping the total thickness constant (ca. 50 nm) and changing the number of ESB/GDC repetitions (N from 1, 10, 20 and 30), the relative thickness of the individual layers (ESB/GDC ratio 1:1 and 6:1), and using undoped CeO_2. Due to the similar lattice parameter at the individual layer (ESB and GDC, ~5.48Å and ~5.44 Å respectively), the multilayer structures arranges ordered structures, with low structural strain, i.e. called superlattice, at low values of N. Electrical properties of the materials in air result from a combination of the starting materials properties and function of the interfaces. The materials under low oxygen partial pressure conditions (~ 10^{-18} atm) present novel properties with an abrupt increase in the electrical conductivity at temperatures above 560-600 °C. This phenomenon is reversible and the resulting materials are stable to ageing treatments and oxidation-reducing cycles.

EXPERIMENTAL

Starting materials were synthesized by solid state reaction of the oxide components Gd_2O_3, CeO_2 for GDC and Er_2O_3 and Bi_2O_3 for ESB in the proper molar ratio. Targets materials for the PLD deposition were pressed as cylindrical pellets by uniaxial load. Dense targets were consolidated by sintering treatments in air high temperatures below the melting point to reach nearly full density. PLD deposition conditions are pO_2 in the deposition chamber was 10^{-3} mbar, the substrate temperature is at a temperature range between 500-700 °C. Target-substrate distance is between 5-7 cm. A KrF excimer laser with wavelength of 248 nm and a pulse width of 25 ns was focused onto a target made of electrolyte oxide materials in order to deposit the target materials onto the substrate and to form the heterostructures by

alternating the materials of the targets. The deposition system was equipped with a multi-target rotating holder. Pure single crystals of (001) MgO and (0001) Al_2O_3 were used as substrates.

The grown films were characterized using various *ex-situ* techniques such as XRD in θ-2θ, ω-θ and reflectivity configurations, transmission electron microscopy (TEM), scanning electon microscopy (SEM), and electrochemical Impedance Spectroscopy (EIS). These were aimed to characterize their structure, crystalline quality, chemical composition and the electrochemical properties.

To optimize for High Resolution TEM (HRTEM) the sample was further thinned by FIB to a thickness of ca. 100 nm

Electrochemical characterization was performed in an in-plane conductivity configuration, where the measuring electrodes are deposited on the film surface.

Discussion

Figure 1 shows a schematic representation of the multilayer arrangement with the typical geometrical parameters: modulation length *(Λ)*, thickness of individual *[ESB/GDC]* bilayers, *GDC/[ESB/GDC]$_N$*, where *N* is the number of bilayers. The number of interfaces formed at the heterostructure is n = 2 x N. The same total thickness of 50 nm was used in this work. MgO single crystal has been selected as a substrate since it shows a remarkably low electrical conductivity at high temperatures. Deposition of ESB/GDC layers directly onto MgO single crystal aims to understand the properties of a new electrolyte material based on Bi_2O_3 without the risk of having electronic-ionic contribution of the substrate. Layer B used is GDC (buffer S´ in figure 1).

Figure 2 shows the X-ray diffraction (XRD) θ-2θ patterns for superlattices GDC/[ESB/GDC]$_N$/MgO having N=1, 10 and 20 with the same overall thickness (50 nm). For N=1, the two close diffraction peaks, which correspond to the (002) reflections of ESB and GDC are visible. For N=10 and N=20 only the average structure peaks could be recognized: satellite peaks are not resolved for the simple reason that they are too close the average structure peaks. The crystallographic quality of heterostructures was estimated by rocking curves in ω–θ XRD configuration, which was centred at the (002) reflections. Rocking curves showed that structural order decreases when increasing the number of interfaces. The inset in figure 2 shows the rocking curve of ESB/GDC superlattice N=20, indicating a full width at half maximum value of about 1.3°. Such value indicates a certain degree of structural disorder in the in-plane arrangement. However, cumulative effect in the GDC/ESB sample can

also be attributed to the large lattice mismatch with the MgO (100) substrate and the GDC buffer layer.

Figure 3 TEM

The N=20 sample was prepared for TEM investigation by thinning with a Focused ion beam (FIB) to a thickness of ca. 200 nm. Figure 3a presents a TEM image of the heterostructure supported on MgO and coated with epoxy for protection during thinning by FIB. Under careful inspection of the dark area representing the heterostructure, the TEM image reveals vertical lines of variations in the image intensity. The relatively weak intensity differences are more readily observed from the line plot in figure 3b obtained from figure 3a. In terms of mass-thickness contrast, the intensity variations (figure 3 a-b) are attributed to the single modulations of the heterostructure. Due to similarity in mass and density of GDC and ESB it is expected that the modulations are only weakly represented by mass-thickness contrast as observed in figure 3a, and ESB is represented by a slightly darker contrast relative to GDC. According to figure 3b, the distance across 10 modulations is ca. 27 nm corresponding to a mean width of 2.7 nm for the modulations. By careful inspection of figure 3a, 20 vertical lines can be identified, corresponding to the number of deposited modulations. The total lamella thickness can be measured to ca. 54 nm (figure 3a), approximately corresponding to the sum of mean modulation distances (20x2.7 nm + 0.5x2.7 = 55.4 nm). It should be noted that the measured total lamella thickness varied by ca. 2 nm for different images. An explanation for this is that the heterostructure-MgO interface is not clearly defined in the images (figure 3a)

Figure 3c presents a HRTEM image of the interface between MgO and the heterostructure at the [001] zone axis of MgO. By imaging at high resolution, the atomic lattice spacing's are observed in terms of phase contrast across the whole image while the mass-thickness contrasts are weaker represented. According to the HRTEM observations (figure 3c) as well as its Fourier transformation (figure 3d), the heterostructure orientation is identical to that of MgO (100). Characteristic lattice spacing lengths of 2.2 Å and 2.7 Å were observed found from the Fourier transformation (fig. 3c) corresponding within the 10% calibration error to the reference [200] lattice spacing of MgO (2.11 Å) and CGO (2.71 Å) and ESB (2.75 Å), respectively. An inverse Fourier transformation (fig. 3e) from the spots corresponding to 2.2 Å in figure 3d, shows that this measured spacing represent MgO in the original image. Similarly, the measured distance of 2.7 Å is attributed both to CGO and EBS (fig. 3f).

It should be noted that, although the cubic structure appears to be well-defined for both the imaged area of MgO and the heterostructure, structure of the interface is less well-defined (figure 3c,e,f), as was also observed in the images at lower resolution (figure 3a). This could be partly expected, since the first deposited modulation is likely to be strained to better

match the difference lattice constant of the MgO support. Figure 3g presents a diffraction pattern of a large area covering both the heterostructure and the MgO support. The diffraction pattern indicates two cubic materials with the same orientation and characteristic lattice spacings of 2.1 Å and 2.7 Å. These observations are all consistent with the HRTEM analysis.

Electrical properties

Electrochemical measurements were carried out by EIS by using pure Au pads electrodes in a symmetric cell configuration. The electrodes were deposited on the thin film heterostructure surface, giving a measure of the in-plane conductivity of the samples. Figure 4 shows electrical performances in the Arrhenius plots of electrical conductivity measured in the 500-750°C temperature range in air for GDC/ESB superlattices with different N (1, 10 ,20 and 30) (figure 4a) and a comparison between GDC/ESB and CeO_2/ESB films at N=20 (figure 4b). Different N corresponds to different modulation length Λ (33, 5, 2.5 and 1.6 nm) for the same overall thickness of ca. 50 nm. Figure 4 also includes conductivity values expected for GDC film, and ESB and δ-Bi_2O_3 (cubic) bulk materials from literature. The measurements in figure 4a were collected both in cooling and in heating ramps, showing reproducibility. Figure 4a shows that ESB/GDC heterostructures present in-air conductivity values comparable to those obtained for the pure materials with activation energy values between 0.8 and 1.1 eV. Particularly, the Arrhenius plot in air shows activation energy of 1.18 eV for superlattices having N=20. Other lattices shows lower activation energy values which are comparable with those observed for pure ionic conductors. Such high values are indeed comparable with both ESB and GDC at low temperatures and indicate that possible absence of order-disorder of oxygen vacancies transition, especially typical of ESB, which occurs below 600°C, leading to activation energy values around 0.65 eV and lower. Figure 4a also shows that a certain increase in conductivity with increasing the number of ESB/GDC interfaces is observed for samples N=1, 10, 20. The films with N=20 showed at 700°C about one order of magnitude larger than the conductivity of GDC deposited on MgO with STO buffer layer (dashed line). This indicates an enhanced conductivity with increasing the number of interfaces and decreasing the thickness of the individual layers. This effect is usually attributed to the presence of a large concentration of defects or strain at the materials interface. Figure 4a shows that a further increase of the number of interfaces in the sample N=30 led to a decrease of conductivity. To clarify the effect of the interfaces on the electrical conductivity electrical conductivity CeO_2/$[ESB/CeO_2]_{20}$/MgO and GDC/$[ESB/GDC]_{20}$/MgO were compared at same thickness and for N=20. Samples GDC/$[ESB/GDC]_{20}$/MgO with ESB:GDC thickness ratio 6:1 and 1:1 are also reported in figure 4b. Decrease in the electrical conductivity for the CeO_2 samples and high activation energy values were observed indicating that ionic conductivity at the later measurement is partially controlled by the ceria component.

Conductivity values registered for CeO_2 sample at high temperatures were comparable to those reported for pure GDC *[M. Mogensen , N.M. Sammes , G. A. Tompsett, Solid State Ionics, 129, 63–94, 2000.].*

Figure 5 shows the Arrhenius plots of electrical conductivity measured in the 500-750°C temperature range at low-oxygen partial pressure (pO2 = 10^{-18} atm) for ESB/GDC superlattices with different N (1, 10, 20 and 30, modulation length Λ= 33, 5, 2.5 and 1.6 nm, respectively) (figure 5a), and samples for N=20 with ESB/GDC 1:1 and 6:1 ratio and CeO_2/[ESB/CeO_2]$_{20}$/MgO (figure 5b). All the samples have the overall thickness of ca. 50 nm. Figure 5a shows that the superlattices showed an abrupt increase in conductivity in the 540-600°C temperature range. Such a transition (transition temp defined as T_t) occurs in the 540-600 °C temperature range. Particularly, superlattices with N=20 show a clear transition at 560°C with an increase of total conductivity of one order of magnitude compared to δ-Bi_2O_3 (dashed line) and two order of magnitude compared to GDC thin film (dashed line) *[K. M. Kant, V. Esposito, N. Pryds, App. Phys. Lett., 97, 143110, 2010]*. At temperature below 540°C the conductivity is comparable to that measured for an ESB pellet. The superlattices with N=1, 10 and 30 showed comparable conductivity of δ-Bi_2O_3 bulk in the 590-750C temperature range *[P. Shuk, H.-D. Wiemhöfer, U. Guth, W. Göpel, M. Greenblat, Solid State Ionics, 89, 179-196, 1996]*. At low pO_2, the activation energy values of the all samples are ≈ 0.8 eV. Such values are usually characteristic for ionic conductivity in bulk and epitaxial films. Figure 5b shows that conductivity of superlattice ESB/CeO_2 is slightly lower than superlattice with N=20 but comparable with the other samples. Such an increase on CeO_2-based sample with respect to the result in air (figure 4b) suggests that some electronic conductivity can occur in such a sample. Sample with N=20 registered the best performances. Sample with ESB/GDC = 6:1 showed again poor conductivity with a continuous degradation of the performances during the 20 hours of measurement. Conversely, all the superlattices with 1:1 ESB/GDC thickness ratio were stable. This is an unexpected phenomenon for Bi_2O_3-based materials which usually are extremely sensitive to reduction. The reversibility of the process also suggests that ESB layers encapsulated in GDC recover their properties in the low temperature regimes below the transition temperature. Irreversible degradation is therefore prevented in the 1:1 ESB/GDC superlattice.

Figure 6 (Brower plot) represent electrical conductivity properties of GDC/[ESB/GDC]$_{20}$/MgO sample as function of the oxygen partial pressure. Different pO_2 values were obtained by mixing O2, H_2 and N_2 in different ratios in dry conditions. Particularly the sample was tested at three different temperatures: at 450 °C < T_t, at 550°C ≈ T_t, and at 650 °C > T_t. The plots show that at low temperature, in the 0.21-10^{-19} atm pO_2 range, the material is mainly ionic with a typical plateau of the conductivity value. The result at 550 °C indicates that the material is ionic up to 10^{-18} atm. However, a transition in the conductivity values was

observed with time. Such a transition is comparable to the phenomena observed in figure 5a, and same conductivity values were reached at the equilibrium. Results at 650 °C show that the material is mainly ionic up to $pO_2=10^{-14}$ atm. For lower values the conductivity abruptly increases of 1 order of magnitude to reach higher values with a typical slope of ¼. Such a slope value is usually associated with the electronic defect formation in doped ceria compounds, and it can be attributed to the GDC component in the superlattice.

Stability

Figure 7

In order to understand the structural stability of the heterostructures, the conductivity as in function of the time was investigated. Figure 7a shows the conductivity of superlattice with N=20 for 550°C, 600°C and 660°C in air. Although the rate of the conductivity decay at 500°C varies dramatically for the ESB bulk reported in literature *[N. Jiang, E.D. Wachsman, J. Am. Ceram. Soc., 82[11), 3057-3064, 1999 and E. D. Wachsman, J. Eur. Ceram. Soc., 24(6), 1281-1285, 2004],* the conductivity for superlattice with N=20 is constant after 95 hours showing high stability and no degradation phenomena. The ionic stability was confirmed from several cycles air/low oxygen partial pressure (fig 4b) at 660°C.

CLAIMS

1. A method for the formation of a thin film multi-layered heterostructure upon a substrate, said method comprising the steps of:

a. providing a substrate;

b. depositing a buffer layer upon said substrate, said buffer layer being a layer of stable ionic conductor (B);

c. depositing a layer A upon said buffer layer, said layer A being a layer of fast ionic conductor (A), said layer A having a thickness (tA) of 20 nm or less;

d. depositing a layer B upon said layer A, said layer B being a layer of stable ionic conductor (B), said layer B having a thickness (tB) of 150 nm or less; and

e. repeating steps c. and d. a total of N times, such that N repeating pairs of layers (A/B) are built up, wherein N is 1 or more.

2. The method according to claim 1, wherein said buffer layer is selected from MgO, NiO, STO, CGO, LAO, NGO and SRO.

3. The method according to any one of the preceding claims, wherein N is 2 or more, such as e.g. 6 or more, 10 or more, 15 or more or 20 or more.

4. The method according to any one of the preceding claims, wherein the fast ionic conductor (A) is selected from erbium-stabilized bismuth oxide (ESB), stabilised cubic bismuth oxide (δ-Bi_2O_3), $(La_{1-x}Sr_x)CoO_3$ (LSC), $(La_{1-x}Sr_x)(Co_{1-y}Fe_y)O_3$,(LSCF), $La_{1-x}Sr_xGa_{1-y}Mg_yO_3$ (LSGM), $AE_{1-x}Sr_xCo_{1-y},Fe_yO_3$ (AE = Ba, Sr), or $Sr_{1-x}Ba_xCe_{1-z}Y_zO_3$.

5. The method according to any one of the preceding claims, wherein the stable ionic conductor (B) is selected from gadolinium doped oxide (GDC or CGO), acceptor doped-ceria compounds and acceptor co-doped-CeO_2 (doped-CeO_2), cubic-phase-stabilised-ZrO_2 or $Ba_{1-x}Sr_xZr_{1-z}Y_zO_3$.

6. The method according to any one of the preceding claims having the following material combinations for A and B:

	A	B
i.	ESB	GDC
ii.	stabilised δ-Bi_2O_3	doped-CeO_2
iii.	LSC and LSCF	doped-CeO_2 and cubic-phase-stabilised-ZrO_2
iv	LSGM	doped-CeO_2 or cubic-phase-stabilised-ZrO_2
v.	$AE_{1-x}Sr_xCo_{1-y},Fe_yO_3$	cubic-phase-stabilised-ZrO_2
vi.	$AE_{1-x}Sr_xCo_{1-y},Fe_yO_3$	doped-CeO_2
vii.	$Ba_{1-x}Sr_xCe_{1-z}Y_zO_3$	$Ba_{1-x}Sr_xZr_{1-z}Y_zO_3$

(AE = Ba, Sr)

7. The method according to any one of the preceding claims, wherein the thin film multi-layered heterostructure has a total thickness of 50 nm or more, preferably 100 nm or more, more preferably 200 nm or more.

8. The method according to any one of the preceding claims, additionally comprising the step of removing the substrate from said thin film multi-layered heterostructure by selective etching of the substrate to access the thin film multi-layered heterostructure from both sides.

9. The method according to any one of the preceding claims, wherein the layer A has a thickness (tA) of 5 nm or less, preferably 3 nm or less.

10. The method according to any one of the preceding claims, wherein the layer B has a thickness (tB) of 100 nm or less, preferably 50 nm or less.

11. A thin film multi-layered heterostructure comprising alternating layers of fast ionic conductor (A) and stable ionic conductor (B), wherein said layer of fast ionic conductor (A) has a thickness of 20 nm or less, and said layer of stable conductor (B) has a thickness of 150 nm or less; said heterostructure comprising N repeating pairs of layers (A/B), wherein N is 4 or more.

12. The thin film multi-layered heterostructure of claim 11, having a total thickness of 50 nm or more, preferably 100 nm or more, more preferably 200 nm or more.

13. The thin film multi-layered heterostructure according to any one of claims 11-12, wherein the layer A has a thickness (tA) of 10 nm or less, preferably 5 nm or less.

14. The thin film multi-layered heterostructure according to any one of claims 11-12, wherein the layer B has a thickness (tB) of 100 nm or less, preferably 50 nm or less.

15. A combination of the thin film multi-layered heterostructure according to any one of claims 11-14 and a substrate, and a buffer layer located between said heterostructure and said substrate, wherein said fast ionic conductor (A) of said heterostructure is located adjacent said buffer layer.

16. Use of a thin film multi-layered heterostructure according to any one of claims 11-14 as a component of a solid-oxide fuel cell (SOFC), solid-oxide electrochemical cell (SOEC), gas-separation membrane, oxygen transport membrane (OTM), sensor or catalyst.

17. A solid-oxide fuel cell (SOFC) comprising the thin film multi-layered heterostructure of any one of claims 11-14 as electrolyte.

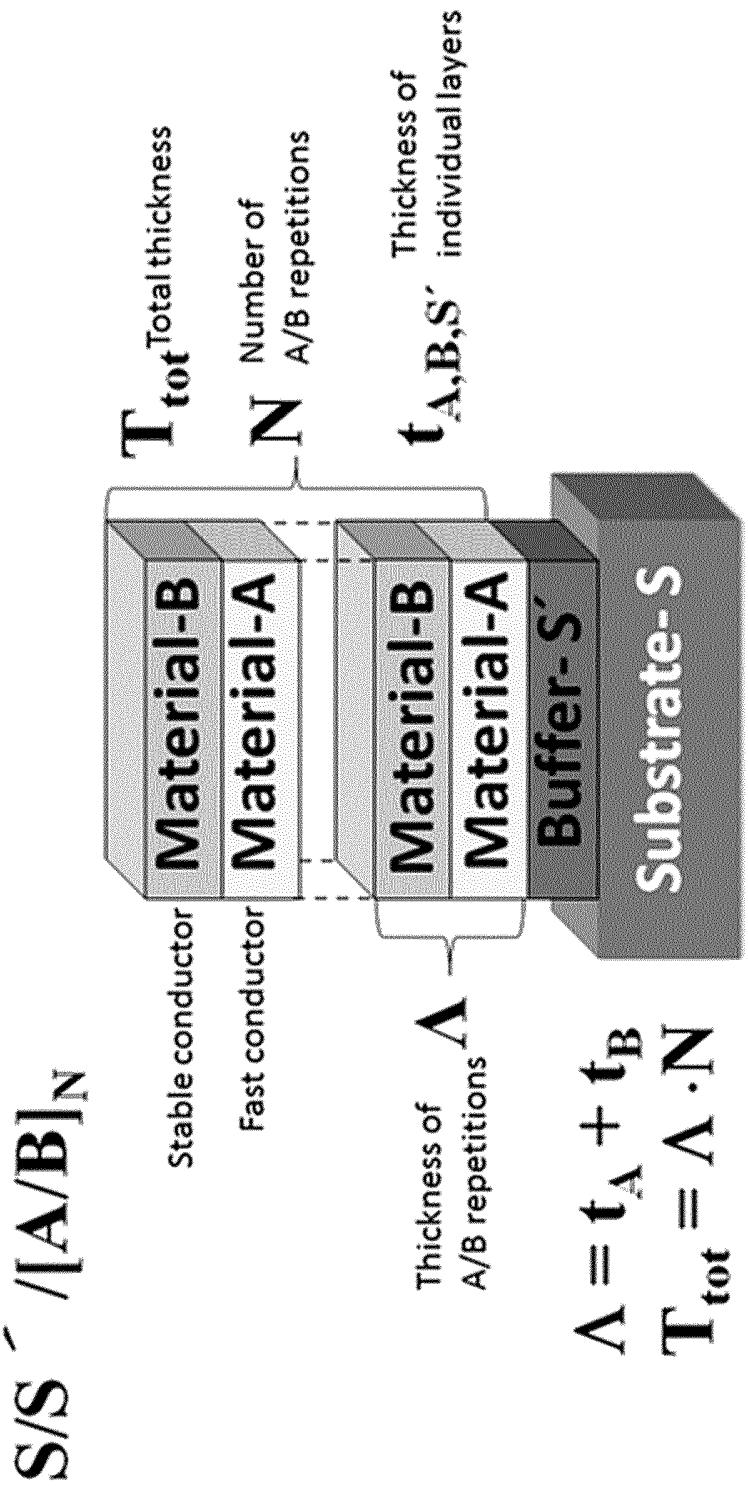
S/S´/[A/B]N
Stable conductor
Fast conductor
Material-B
Material-A
Material-B
Material-A
Buffer- S´
Substrate- S
Thickness of A/B repetitions Λ
Λ = tA + tB
Ttot = Λ .N
Ttot Total thickness
N Number of A/B repetitions
tA,B,S´ Thickness of individual layers

FIG. 1

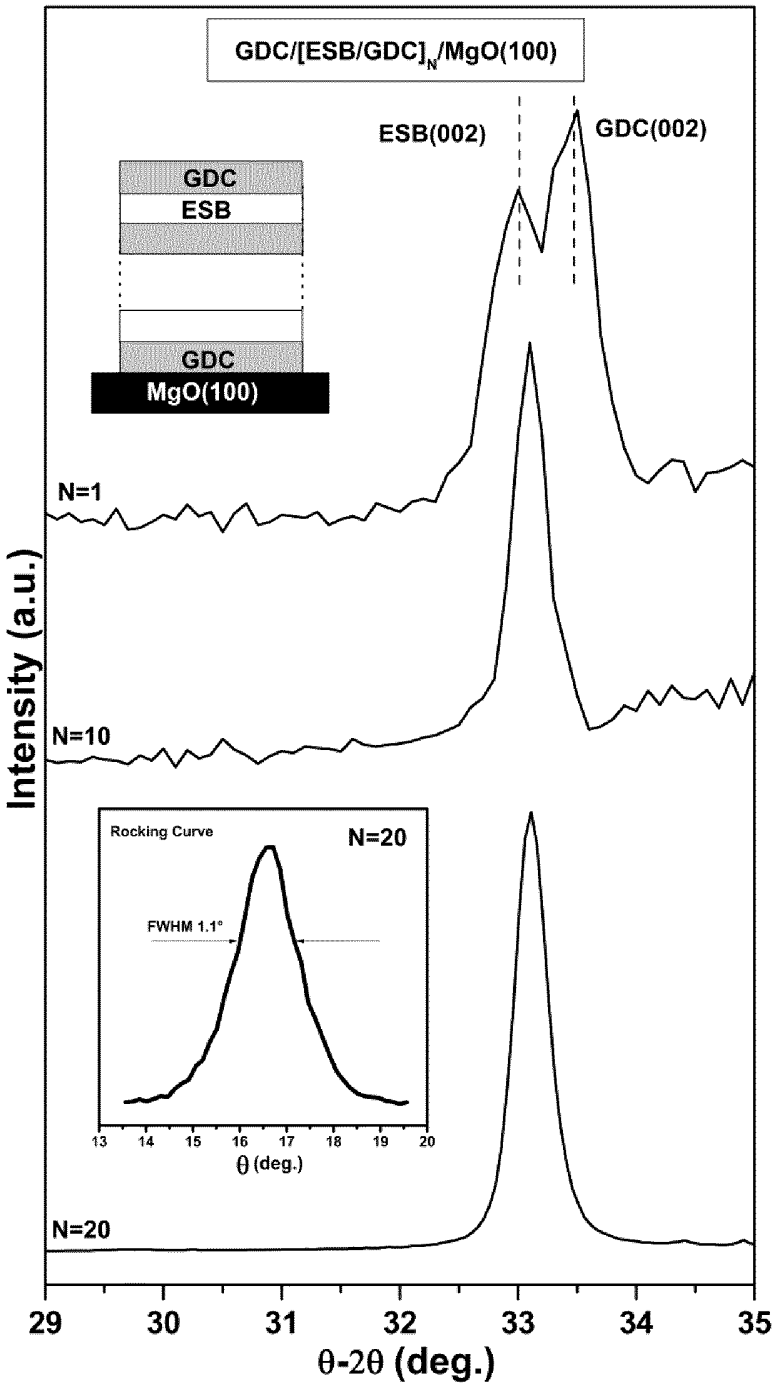
GDC/[ESB/GDC]N/MgO(100)
ESB(002)
GDC(002)
GDC
ESB
GDC
MgO(100)
N=1
N=10
N=20
Intensity (a.u.)
Rocking Curve
N=20
FWHM 1.1°
13 14 15 16 17 18 19 20
θ (deg.)
29 30 31 32 33 34 35
θ-2θ (deg.)

FIG. 2

FIG. 3

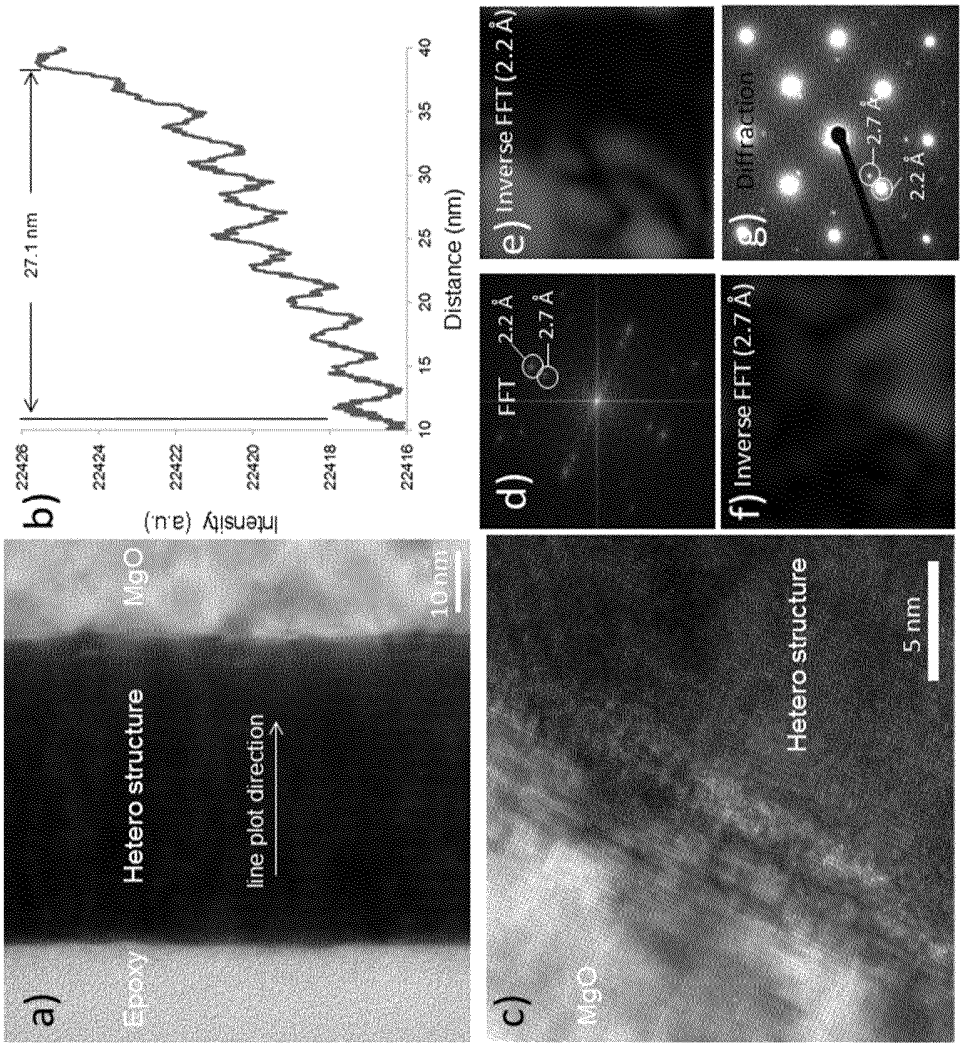
a)
Epoxy
Hetero structure
MgO
line plot direction
10 nm
b)
27.1 nm
Intensity (a.u.)
Distance (nm)
c)
MgO
Hetero structure
5 nm
d)
FFT
2.2 Å
2.7 Å
e) Inverse FFT (2.2 Å)
f) Inverse FFT (2.7 Å)
g) Diffraction
2.7 Å
2.2 Å

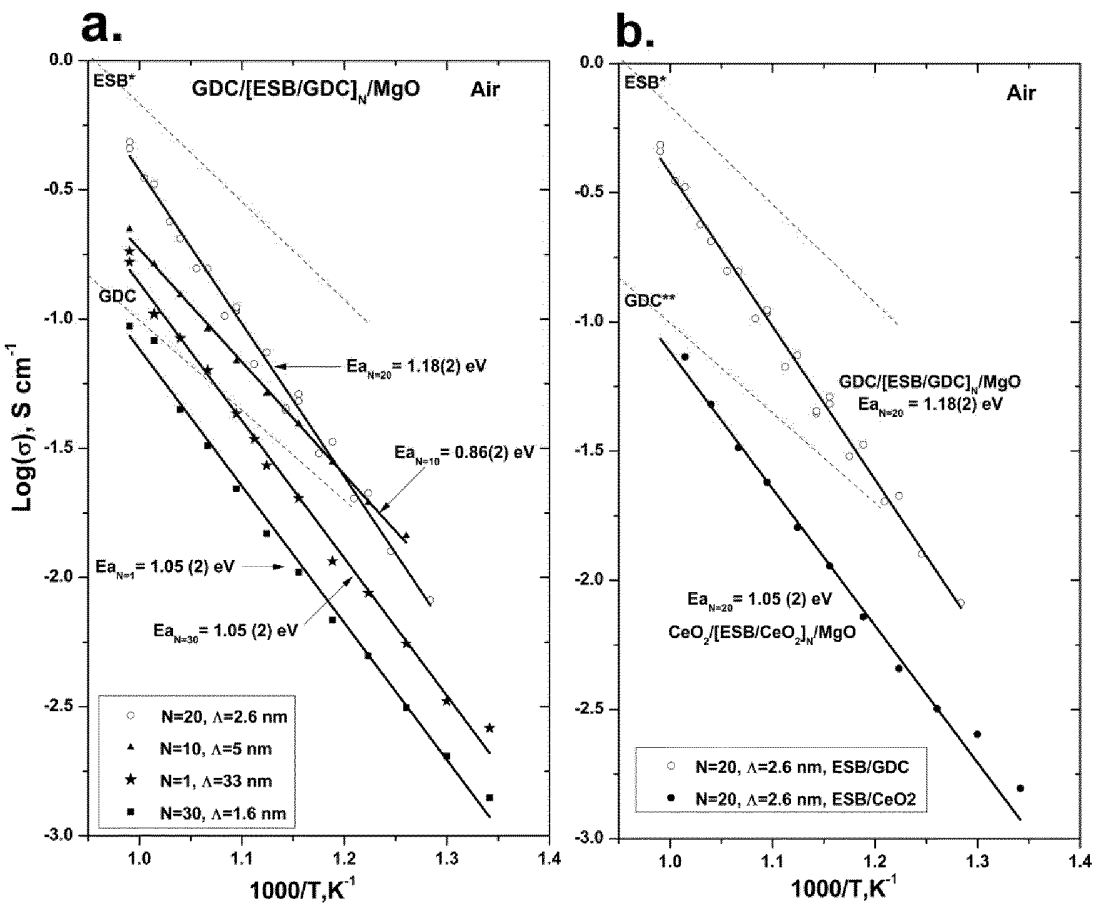
a.
b.
ESB*
GDC
GDC/[ESB/GDC]N/MgO
Air
Ea N=20 = 1.18(2) eV
Ea N=10 = 0.86(2) eV
Ea N=1 = 1.05 (2) eV
Ea N=30 = 1.05 (2) eV
N=20, Λ=2.6 nm
N=10, Λ=5 nm
N=1, Λ=33 nm
N=30, Λ=1.6 nm
Log(σ), S cm-1
1000/T,K-1
GDC**
Ea N=20 = 1.05 (2) eV
CeO2/[ESB/CeO2]N/MgO
N=20, Λ=2.6 nm, ESB/GDC
N=20, Λ=2.6 nm, ESB/CeO2

FIG. 4

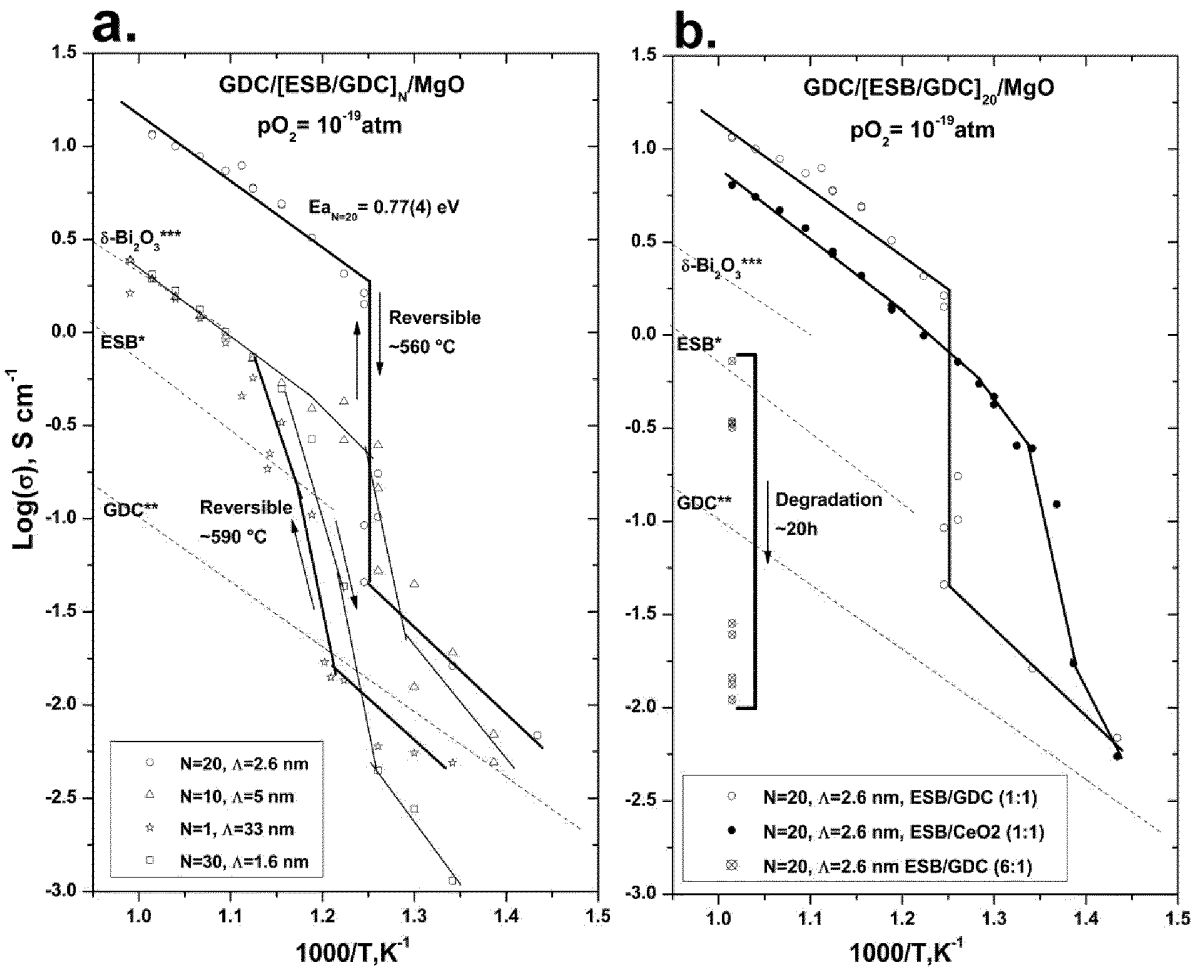
a.
GDC/[ESB/GDC]N/MgO
pO2= 10-19atm
EaN=20= 0.77(4) eV
δ-Bi2O3***
ESB*
GDC**
Reversible
~560 °C
Reversible
~590 °C
N=20, Λ=2.6 nm
N=10, Λ=5 nm
N=1, Λ=33 nm
N=30, Λ=1.6 nm
Log(σ), S cm-1
1000/T,K-1
b.
GDC/[ESB/GDC]20/MgO
pO2= 10-19atm
δ-Bi2O3***
ESB*
GDC**
Degradation
~20h
N=20, Λ=2.6 nm, ESB/GDC (1:1)
N=20, Λ=2.6 nm, ESB/CeO2 (1:1)
N=20, Λ=2.6 nm ESB/GDC (6:1)
1000/T,K-1

FIG. 5

FIG. 6

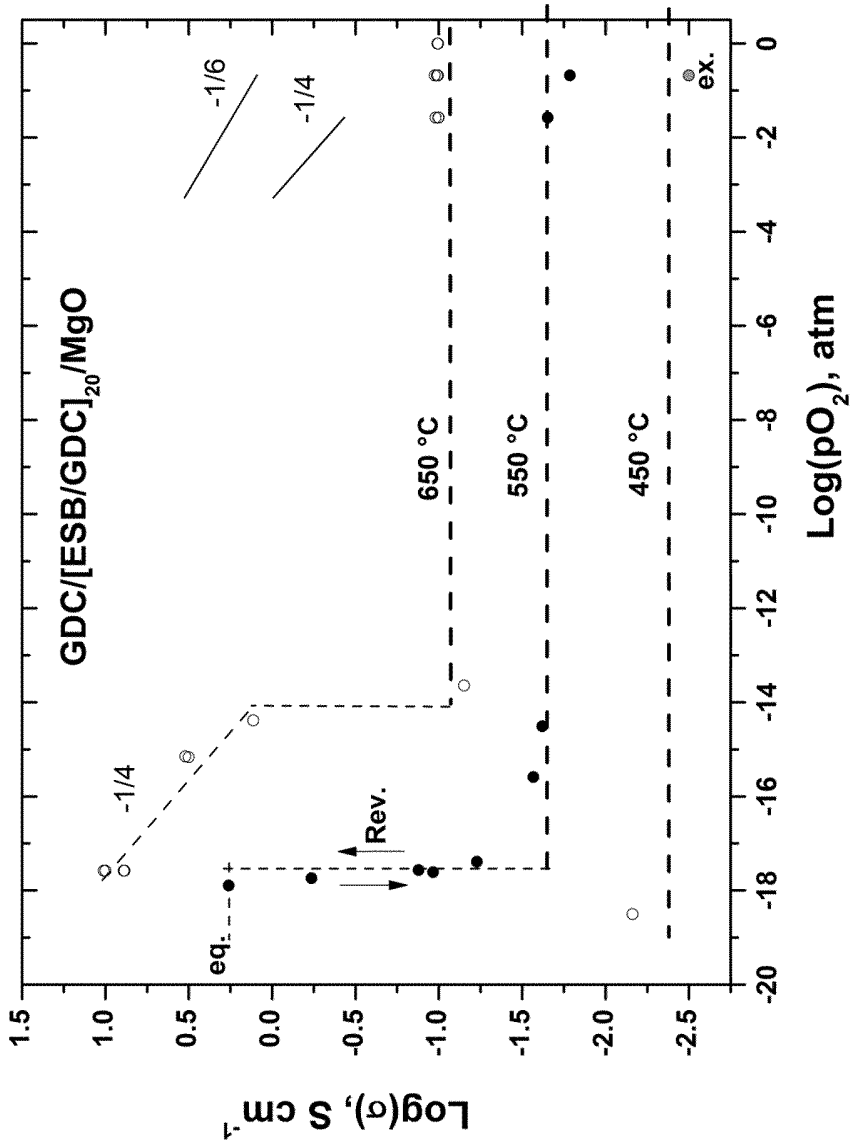
GDC/[ESB/GDC]20/MgO
-1/6
-1/4
-1/4
650 °C
550 °C
450 °C
eq.
Rev.
ex.
Log(σ), S cm-1
Log(pO2), atm
1.5
1.0
0.5
0.0
-0.5
-1.0
-1.5
-2.0
-2.5
0
-2
-4
-6
-8
-10
-12
-14
-16
-18
-20

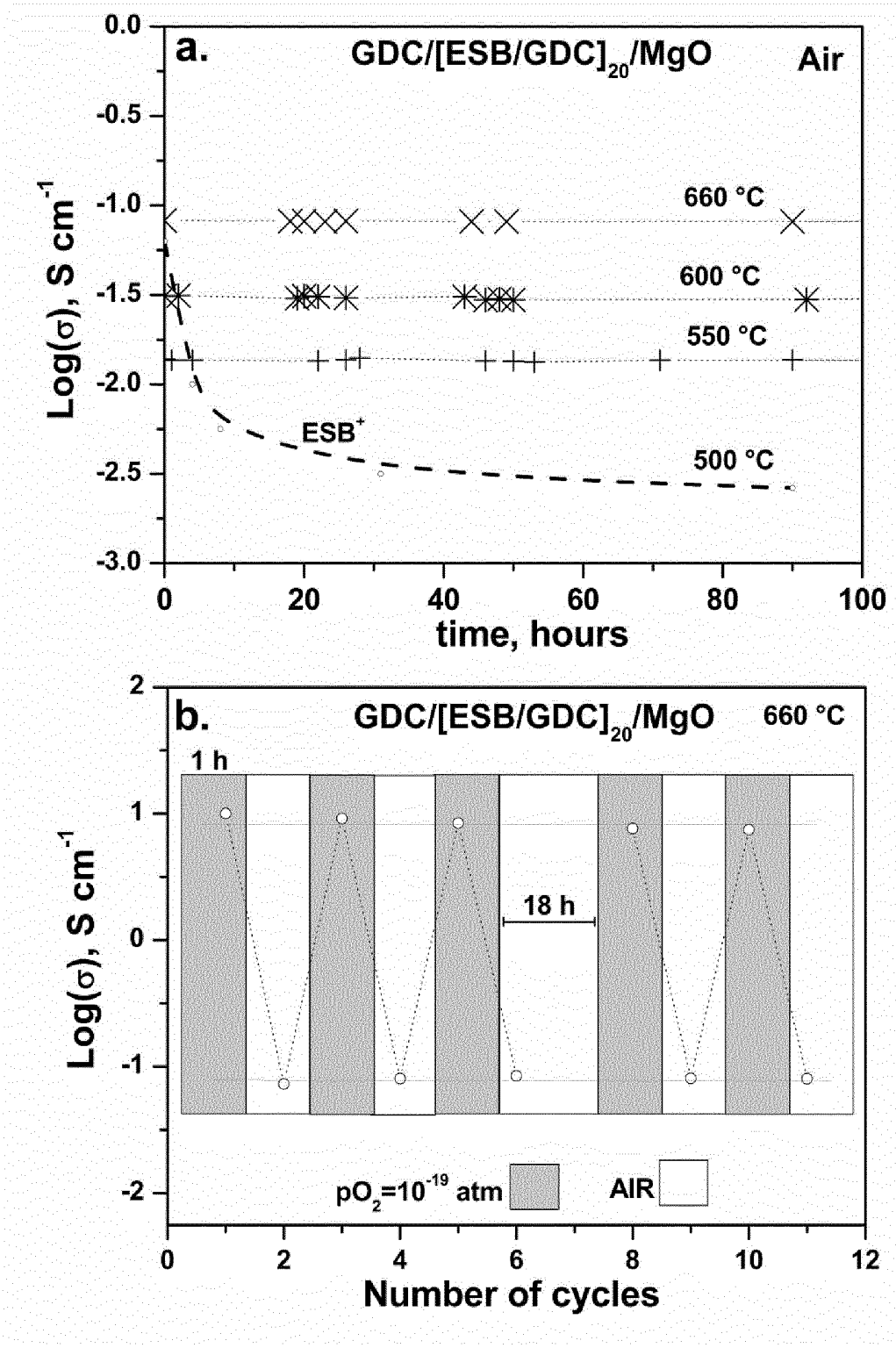
a.
GDC/[ESB/GDC]20/MgO
Air
660 °C
600 °C
550 °C
500 °C
ESB+
Log(σ), S cm-1
time, hours
b.
GDC/[ESB/GDC]20/MgO
660 °C
1 h
18 h
pO2=10-19 atm
AIR
Log(σ), S cm-1
Number of cycles

FIG. 7

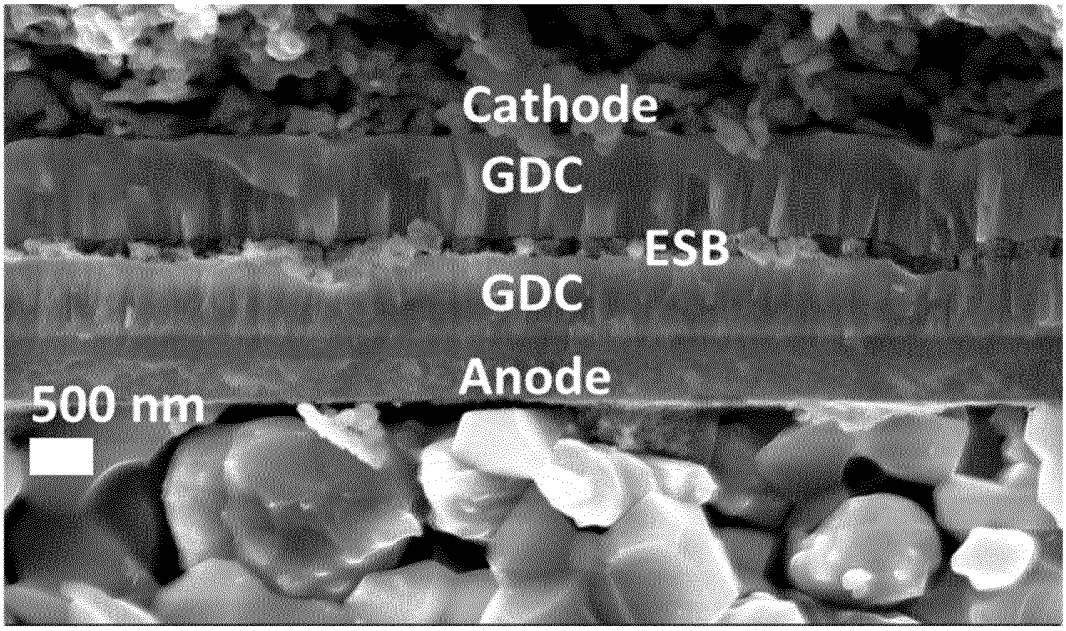
Cathode
GDC
ESB
GDC
Anode
500 nm

FIG. 8

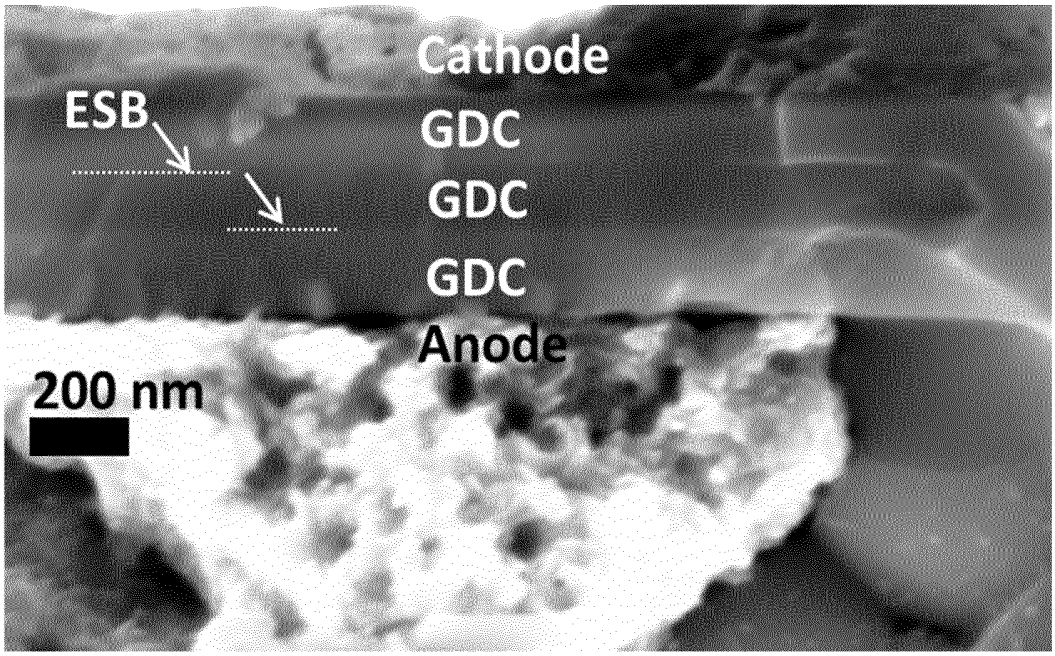
ESB
Cathode
GDC
GDC
GDC
Anode
200 nm

FIG. 9

INTERNATIONAL SEARCH REPORT

International application No
PCT/EP2014/064812

A. CLASSIFICATION OF SUBJECT MATTER
INV. H01M8/12 H01M8/02
ADD.

According to International Patent Classification (IPC) or to both national classification and IPC

B. FIELDS SEARCHED

Minimum documentation searched (classification system followed by classification symbols)
H01M

Documentation searched other than minimum documentation to the extent that such documents are included in the fields searched

Electronic data base consulted during the international search (name of data base and, where practicable, search terms used)
EPO-Internal, WPI Data

C. DOCUMENTS CONSIDERED TO BE RELEVANT

Category*	Citation of document, with indication, where appropriate, of the relevant passages	Relevant to claim No.
X	US 2004/096572 A1 (CHEN XIN [US] ET AL) 20 May 2004 (2004-05-20) claims 1-17 paragraphs [0028], [0029], [0030], [0035], [0036], [0038], [0039] figures 1-10 -----	1-10
X	US 6 645 656 B1 (CHEN XIN [US] ET AL) 11 November 2003 (2003-11-11) claims 1-9 figures 1-9 column 3, line 57 - column 4, line 22 column 5, line 54 - column 6, line 28 column 6, line 45 - column 7, line 30 ----- -/--	1-10

[X] Further documents are listed in the continuation of Box C.

[X] See patent family annex.

* Special categories of cited documents :

"A" document defining the general state of the art which is not considered to be of particular relevance

"E" earlier application or patent but published on or after the international filing date

"L" document which may throw doubts on priority claim(s) or which is cited to establish the publication date of another citation or other special reason (as specified)

"O" document referring to an oral disclosure, use, exhibition or other means

"P" document published prior to the international filing date but later than the priority date claimed

"T" later document published after the international filing date or priority date and not in conflict with the application but cited to understand the principle or theory underlying the invention

"X" document of particular relevance; the claimed invention cannot be considered novel or cannot be considered to involve an inventive step when the document is taken alone

"Y" document of particular relevance; the claimed invention cannot be considered to involve an inventive step when the document is combined with one or more other such documents, such combination being obvious to a person skilled in the art

"&" document member of the same patent family

Date of the actual completion of the international search	Date of mailing of the international search report
15 October 2014	22/10/2014

Name and mailing address of the ISA/	Authorized officer
European Patent Office, P.B. 5818 Patentlaan 2 NL - 2280 HV Rijswijk Tel. (+31-70) 340-2040, Fax: (+31-70) 340-3016	Reich, Claus

2

Form PCT/ISA/210 (second sheet) (April 2005)

INTERNATIONAL SEARCH REPORT

International application No
PCT/EP2014/064812

C(Continuation). DOCUMENTS CONSIDERED TO BE RELEVANT

Category*	Citation of document, with indication, where appropriate, of the relevant passages	Relevant to claim No.
X	WO 2012/145531 A2 (BROARD OF REGENTS OF THE UNIVERSITY OF TEXAS SYSTEM [US]; CHEN CHONGLI) 26 October 2012 (2012-10-26) paragraphs [0025] - [0028]	11-17
A	WO 2010/045329 A2 (UNIV FLORIDA [US]; WACHSMAN ERIC D [US]; YOON HEESUNG [US]; LEE KANG-T) 22 April 2010 (2010-04-22) claims 1-21	7
A	US 5 985 476 A (WACHSMAN ERIC D [US] ET AL) 16 November 1999 (1999-11-16) claims 1-25 column 4, paragraph 48 - column 5, paragraph 57	11-17
A	JP H09 63603 A (NIPPON TELEGRAPH & TELEPHONE) 7 March 1997 (1997-03-07) claims 1-4	1-17
A	WO 2008/146927 A1 (HONDA MOTOR CO LTD [JP]; KOMIYA TERUAKI [JP]) 4 December 2008 (2008-12-04) claims 1-9; figure 3	1-17
A	US 2011/003235 A1 (HWANG CHANG-SING [TW] ET AL) 6 January 2011 (2011-01-06) paragraph [0074]	1-17
A	WO 2008/050437 A1 (TOTO LTD [JP]; KAWAKAMI AKIRA [JP]; MATSUOKA SATOSHI [JP]; WATANABE NA) 2 May 2008 (2008-05-02) claims 1-12	1-17

2

INTERNATIONAL SEARCH REPORT

Information on patent family members

International application No
PCT/EP2014/064812

Patent document cited in search report	Publication date	Patent family member(s)	Publication date
US 2004096572 A1	20-05-2004	NONE	
US 6645656 B1	11-11-2003	NONE	
WO 2012145531 A2	26-10-2012	NONE	
WO 2010045329 A2	22-04-2010	CA 2740293 A1	22-04-2010
		EP 2338201 A2	29-06-2011
		JP 2012506127 A	08-03-2012
		KR 20110086016 A	27-07-2011
		US 2011200910 A1	18-08-2011
		WO 2010045329 A2	22-04-2010
US 5985476 A	16-11-1999	US 5725965 A	10-03-1998
		US 5985476 A	16-11-1999
JP H0963603 A	07-03-1997	JP 3259756 B2	25-02-2002
		JP H0963603 A	07-03-1997
WO 2008146927 A1	04-12-2008	NONE	
US 2011003235 A1	06-01-2011	TW 201103185 A	16-01-2011
		US 2011003235 A1	06-01-2011
WO 2008050437 A1	02-05-2008	CN 101558520 A	14-10-2009
		DE 112006004086 T5	10-09-2009
		WO 2008050437 A1	02-05-2008